AN INVESTIGATION INTO THE EFFECTS OF REYNOLDS NUMBER AND TURBULENCE UPON THE CALIBRATION OF 5-HOLE CONE PROBES

H.P. Hodson and R.G. Dominy,
Whittle Laboratory,
Cambridge University, U.K.

SUMMARY

The effects of changes in Reynolds number upon the calibrations of four different type of 5-hole cone probes have been studied. Three different cone angles (45°, 60° and 90°) and two hole geometries were investigated. The probes were calibrated at the exit from a transonic nozzle over a range of Reynolds numbers ($7 \times 10^3 < Re_p < 80 \times 10^3$) with additional information being obtained by calibrating in a low speed open jet. The effects of compressiblity and free-stream turbulence upon the sensitivity to Reynolds number are also discussed.

Two distinct Reynolds number effects have been identified. Flow separation affects the calibrations at relatively low Reynolds numbers while the structure of the flow around the sensing holes appears to be responsible for the second effect, which is greatest when the probe is nulled.

INTRODUCTION

The Reynolds number of a 5-hole probe

$$Re_p = \frac{\rho V d}{\mu}$$

may be adequately defined in terms of the local free stream conditions and the overall diameter of the probe. Likewise, in turbomachinery applications, the Reynolds number of the bladerow under investigation

$$Re_c = \frac{\rho V c}{\mu}$$

may be defined using either inlet (compressor) or exit (turbine) flow conditions and a characteristic length scale, for example, the chord c. In the case of measurements being conducted at exit from a turbine cascade, therefore, the probe and cascade Reynolds numbers are related by the simple expression

$$Re_p = Re_c \frac{d}{c}$$

while in the case of measurements behind a compressor,

$$Re_p = Re_c \frac{d}{c} \frac{V_{exit}}{V_{inlet}}$$

In either situation, once the operating conditions are determined, the probe Reynolds number is determined solely by the relative length scales (d/c) of the probe and blade row.

Typical values of cascade and probe Reynolds numbers are given in Tables Ia and Ib for high an low speed experiments carried out at the Whittle Laboratory. Since low speed cascades tend to be much larger than their high speed counterparts, the Reynolds numbers of low speed probes tend t be much less than those probes used in high speed cascades at equivalent chord-based Reynolds numbers. In all cases, however, it is likely that probe Reynolds numbers will lie in the range fron 1×10^3 to 100×10^3.

Table Ia Reynolds numbers for a Sonic cascade with a chord of 50mm, a probe of 2mm dia. and ambient temperature

Static pressure	Re_c	Re_p
1/30 atm	0.35×10^5	1×10^3
1/3 atm	3.5×10^5	14×10^3
1 atm	11×10^5	42×10^3
2 atm	22×10^5	84×10^3

Table Ib Reynolds numbers for a Low Speed cascade with a probe of 2mm dia. and a chord of 250mm

	Re_c	Re_p
Atmospheric Temperature and Pressure	5×10^5	4×10^3

In the past, the effects of Reynolds number upon probe performance have received little attention i the open literature. This is perhaps because it is only recently that minature probes have become commonplace and it is these that are most likely to exhibit problems when operating over the large range of Reynolds numbers which is often possible in high speed facilities.

Krause and Dudzinski [1] examined the effects of Reynolds number upon the yaw and pitch sensitivity of a 5-hole pyramid probe (fig. 1a). The probe had an included angle at the tip of 90° and, since the probe was fabricated by bundling tubes together, the pressure tappings faced forwards into the flow. Over the range of Reynolds numbers investigated ($3 \times 10^3 < Re_p < 40 \times 10^3$ based upon overall tip width), the changes in calibration coefficient represented errors in the yaw and pitch of 1.5° and 3° respectively at a yaw angle of 10° and a pitch angle of 20°. The variation i indicated angle was greatest at the lowest Reynolds numbers and appeared to be neligible at the highest.

Sitram et. al. [2] report the performance of a similarly manufactured probe, albeit with a hemispherical head, over a limited range of Reynolds numbers from 2×10^3 to 7×10^3. The probe was intended for low speed measurements. With the probe at a yaw angle of 10° and zero pitch, their results show that there are potential errors of 0.2° in the yaw measurement over the restricted range of Reynolds numbers. The variation in indicated static pressure was equivalent to 5 percent the dynamic pressure. These errors were only slightly increased when the pitch was also set to 10

Smith and Adcock [3] were also concerned with a pyramid probe. In their study, the probe had a 66° included angle and pressure tappings drilled perpendicular to the faces of the pyramid (fig. 1b). They studied the influence of Reynolds number upon the angular sensitivity, which was assumed to be linear for angles in the range ±4°. The minimum Reynolds number for the tests was approximately $25x10^3$. Although there are few data points, the results show that the effects of Reynolds number are limited to values below $100x10^3$.

Wallen [4] calibrated a cone probe at three Reynolds numbers, namely $25x10^3$, $43x10^3$ and $72x10^3$. The probe had an included tip angle of 60° and the side pressure tappings were drilled perpendicular to the surface of the cone (Fig. 2b). Although not obvious from the calibration curves that he presented, Wallen concluded that over the range of Reynolds numbers investigated and at pitch and yaw angles of 10°, the variations of the calibration coefficients represented errors of approximately 1.2° of yaw and pitch. In the measurement of the stagnation and static pressures, the variations were equivalent to 0.3 and 1.7 percent of the dynamic head respectively. In the case of a similar cone probe, albeit with an included angle of 70°, Koschel and Pretzsch [5] concluded that the effects of Reynolds number are negligible for probe Reynolds numbers in the range from $37x10^3$ to $82x10^3$. However, a close inspection of their data reveals indicated errors of approximately 0.8° at 15° of yaw or pitch over the range investigated. There are no comments upon the sensitivity of the static and stagnation pressure measurements.

At lower Reynolds numbers ($2x10^3 < Re_p < 20x10^3$), Novak [6] observed that for a nulled 90° cone probe with forward facing pressure tappings (fig. 2a), the indicated static pressure varied by approximately 5 percent of the true dynamic pressure.

The published literature, though lacking physical insight, clearly shows that that the calibrations of 5-hole probes are influenced by Reynolds number; that there is probably a limit above which there is no influence; that this limit is probably above the values given as examples in Table I and that the extent of the influence is related to the probe design.

The present study is exclusively concerned with 5-hole cone probes, since these appear to be the type most widely employed. Probes of differing included angles (45° to 90°) and hole configurations are examined. The effects of Reynolds number and the effects of turbulence and compressiblity upon the sensitivity to Reynolds number are reported.

EXPERIMENTAL FACILITIES

Transonic Nozzle

The high speed calibrations of the probes were carried out using the Transonic Cascade Test Facility [7] of the Whittle Laboratory. This is a closed circuit, variable density ($0.04 < \rho < 2.4$ kg/m^3) wind tunnel in which the Mach number and Reynolds number can be varied independently while the temperature is maintained at ambient conditions.

For the purposes of the present investigation, the working section was fitted with a transonic nozzle (fig. 3) similar to that developed by Baines [8]. The upper and lower walls of the nozzle are perforated so as to provide continuous acceleration over a range from subsonic to supersonic exit Mach numbers without requiring a change of geometry. The extended side walls are suitable for double pass Schlieren photography. The stagnation pressure was measured in the upstream plenum and a row of pressure tappings was arranged at mid-height along the reflecting side wall.

The facility includes a computer controlled 5-axis traversing and data acquisition system. During calibration, the yaw and pitch angles can be varied in the range ±80°. The 5-hole probe under investigation was positioned in the centre of the nozzle exit plane (as defined by the upper and lower porous walls), at the same axial location as one of the side wall pressure tappings.

In order to calibrate the transonic nozzle, a needle static pressure probe was placed in the calibration nozzle and traversed along the axis of the nozzle at a range of Mach numbers. The static pressures so measured were in excellent agreement with those indicated by the side wall static pressure tappings. Therefore, in the calibration results which follow the static pressure local to the probe is taken to be equal to that measured by the side wall pressure tapping at the same axial location.

Fig. 4 shows the effect of changing the back pressure on the Mach number distribution within th nozzle. The acceleration is continuous at each condition shown. Schlieren photographs were alsc taken of the flow in the nozzle while the needle static pressure probe was in place. An example is shown in Fig. 5. Mach numbers determined from the angles of the Mach lines which originate from the holes in the porous top and bottom walls are also plotted in Fig. 4. For equivalent conditions, the maximum difference in Mach number is equal to 0.006.

Low Speed Nozzle

In addition to the high speed tests, a limited set of low speed tests were performed using a conventional, atmospheric exit, low speed wind tunnel fitted with a convergent nozzle at exit. Lo flow conditions were determined using a conventional pitot-static pressure probe.

PROBE GEOMETRIES

Cone probes of four different designs were calibrated as part of the study. Their identification co cone angle, diameter and hole configuration (fig. 2) are given in Table II.

Table II Probe Designs

Probe No.	Cone Angle	Hole Configuration	Diameter (mm)
501	60°	Forward facing	2.06
504	60°	Perpendicular	3.29
506	90°	Perpendicular	3.29
507	45°	Perpendicular	3.29
514	60°	Forward facing	34.5

The hole configuration, which is designated as either *forward facing* or *perpendicular*, refers to whether the axes of the yaw and pitch holes are parallel to the axis of the probe and so face forwa into the flow or are perpendicular to the surface of the cone.

The smallest diameter of the high speed probes was 2.06mm while the larger ones had a diamete 3.29mm in order to improve the probe response during the calibrations. The largest probe (no. 5 was used to investigate the effect of turblence on the Reynolds number sensitivity at low speed. had previously been used in an investigation which included a flow visualisation study of probe aerodynamics [10]. The probes were mounted on stings. so as to eliminate any problems associa with stem blockage. The probe blockage was less than 0.1 percent of the nozzle exit area in all cases.

CALIBRATION AND PRESSURE COEFFICIENTS

Fig. 6 illustrates the convention used to number the 5-hole probe pressure tubes. The following definitions are used for the calibration coefficients presented in this paper

Yaw Angle $\frac{p_2 - p_3}{p_1 - p_{av}}$

Pitch Angle $\frac{p_4 - p_5}{p_1 - p_{av}}$

Stagnation Pressure $\frac{P_o - p_1}{p_1 - p_{av}}$

Dynamic pressure $\frac{P_o - p_s}{p_1 - p_{av}}$

where p_{av} is the mean of the pressures measured by the side holes, that is

$$p_{av} = (p_2 + p_3 + p_4 + p_5) / 4.$$

In addition to the calibration coefficients, the pressures from each hole (p_i, i=1..5) are presented as non-dimensional pressure coefficients of the form

Pressure Coefficient No. i $\frac{p_i - P_o}{P_o - p_s}$

RESULTS AND DISCUSSION

In the following sections, the effects of Reynolds number are presented in terms of contoured surfaces where the height represents the value of the pressure or calibration coefficient, and elevations of those same surfaces at different Reynolds numbers. The former is used to highlight the areas of significance while the latter serve to better illustrate the magnitude of the effects studied.

The results presented in this paper have been obtained at zero pitch angle since the authors were mainly concerned with the determination of the mechanisms associated with Reynolds number effects and the range over which they existed. The combined effects of pitch and yaw can easily be inferred from the results obtained at zero pitch angle.

Effects of Reynolds Number

This section presents the results obtained by calibrating the probes over a range of Reynolds numbers, extending from 7×10^3 to approximately 80×10^3 at Mach 0.9.

60°, forward facing, cone probe. The pressures measured by the stagnation or centre hole (hole 1) at different yaw angles and Reynolds numbers are plotted in fig. 7 in the form of a pressure coefficient. The contours of the pressure coefficient in Fig. 7a show that it is independent of Reynolds number over the range investigated. Fig. 7b confirms that this is the case. The result is typical of many probes. The thickness of the envelope of the surface is shown by Fig. 7b to be less than 0.1 percent of the free stream dynamic pressure (P_o-p_s), which corresponds to the overall measurement accuracy of the system at low pressures.

The sensitivity of one of the yaw tubes (hole 2) of the same probe to changes in Reynolds number and yaw may be deduced from the results presented in Fig. 8. Unlike the stagnation hole, the response of the yaw holes is clearly affected by changes in the Reynolds number. There are two regions of significant influence. The first is found below Reynolds numbers of approximately 21×10^3 at large negative yaw angles, when the measured pressure begins to fall with reducing

Reynolds number. This effect is most pronounced at a yaw angle of -20° and a Reynolds number of $15x10^3$. The low pressure is due to the influence of a separation bubble which, as the photograph of Fig. 10 (from ref [10]) shows, originates near the leading edge of the probe and extends over the forward part of the hole at even modest yaw angles. The apparent recovery of pressure at lower Reynolds numbers is believed to be a consequence of the changing nature of the interaction of the separation with the pressure hole. The results of Gaillard [9] show that although the pressure measured by the downwind yaw hole of a 45° probe at similar Reynolds numbers recovers when stall takes place, a 60° probe does not exhibit the same phenomena at the yaw angles encountered here. Therefore, it is unlikely that it indicates full separation.

The second region of operation where the influence of Reynolds number is significant occurs when the magnitude of the yaw angle is less that 8°. At high Reynolds numbers, Fig. 8a shows that the pressure coefficient is insensitive to yaw between 0° and 4° while at small negative yaw angles, the sensitivity is much greater than the normal value. At Reynolds numbers below about $50x10^3$, the asymmetry is less pronounced and at the lowest Reynolds numbers, it has virtually disappeared. Fig. 9 shows the response of the second yaw hole (hole 3) over the same range of yaw angles and Reynolds numbers. A comparison of figs. 8 and 9 show that the symmetry of the probe excellent and that the features noted in fig. 8 are not a peculiarity of only one hole.

The data obtained from one of the pitch holes (hole 4) is plotted in fig. 11. Although not presented the response of the second pitch hole (hole 5) was very similar to that of the first. At large positive or negative yaw angles, the influence of Reynolds number is only just discernable in either fig. 11a or 11b. However, at small yaw angles, Reynolds number effects are clearly evident. The region of influence extends from a Reynolds numbers of $13x10^3$ to the highest values tested. With the probe nulled, fig. 11b indicates that the variation in pressure is equivalent to 10 percent of the dynamic pressure and is therefore similar in magnitude to the variations observed for the yaw holes (figs 8b and 9b) over the same range of Reynolds numbers. Thus, it might be concluded that the same mechanism is responsible in each case.

So far, the discussion has been concerned with the response of individual pressure holes, primarily because it is often difficult to identify the different phenomena using the calibration coefficients which, by necessity, are determined from the pressures of several holes. The form of the presentation chosen for the yaw coefficient data of fig. 12, for the data of fig. 13 (dynamic pressure coefficient) and similar figures is identical to that of the preceeding pressure coefficient plots. A consistant format has been adopted specifically to aid interpretation of the data. This is inspite of the fact that in practice, the yaw angle is unknown until the calibration has been applied to the experimental data. Care must therefore be taken when analysing the stagnation pressure and dynamic pressure coefficient data so presented since the coefficients themselves are dependent upon the yaw angle irrespective of any Reynolds number influence.

Fig. 12 illustrates the influence of Reynolds number and yaw upon the yaw coefficient. In fig. 12a, the contour interval represents changes in yaw angle of approximately 2°. The yaw coefficient clearly exhibits the effects of flow separation at high yaw angles for Reynolds numbers less than approximately $21x10^3$, with the variation leading to a possible error of approximately 5°. At small yaw angles and by virtue of a fortuitous combination of events over the entire range of Reynolds numbers, the potential error appears to be less than 2°, approximately half that indicated by figs. 8 and 9. For probes which have more asymmetry than the present one, this may not be the case.

The dynamic pressure coefficient for the same probe is plotted in fig. 13. In fig. 13a, where the contour interval represents approximately 1 percent of the true dynamic head, the influence of separation at low Reynolds numbers is visible even at modest yaw angles. At ±20° of yaw, changing the Reynolds number may produce errors of approximately 6 percent in the measurement of dynamic pressure due to the presence of separated flow. In practice, the yaw angle will itself be in error by upto 5°, which will fortuitously reduce the error in dynamic pressure measurement to approximately 3 percent.

When the yaw angle is small, the influence observed throughout the range of Reynolds numbers in figs 8, 9 and 11 can also be seen in fig. 13. With the probe nulled, there is a potential error of approximately 20 percent when measuring the dynamic pressure. This is approximately four times that observed by Novak [6] for a 90° cone probe which also had forward facing holes.

The influence of Reynolds number and yaw upon the measurement of stagnation pressure has already been discussed with reference to fig. 7, which showed that the pressure coefficient based on the pressure measured by the centre hole was a function only of the flow angle, that is, it was not affected by changes in Reynolds number. However, the value of the correction ($P_O - p_1$) to be applied to the measured value p_1 in order to obtain the true stagnation pressure P_O will be subject to the same relative errors as the true dynamic pressure ($P_O - p_S$). This is because the error essentially lies in the accuracy of the psuedo dynamic pressure ($p_1 - p_{av}$), which forms the denominator of relevant coefficients.

<u>60°, perpendicular, cone probe.</u> The above discussion was concerned with a 60° cone probe which was constructed with forward facing pressure tubes. This section presents some of the results obtained by calibrating a probe with the same cone angle but with the pressure holes drilled normal to the surface of the cone. As a result of this change, the pressure holes on the cone surface are located further from the probe tip. They also occupy a much smaller proportion of the surface for a given relative hole diameter.

The dynamic pressure coefficient for the new probe is presented in fig. 14. The contour interval in fig. 14a again represents approximately 1 percent of the true dynamic pressure. The lower overall level of the coefficient indicates that the sensitivity to dynamic pressure has been improved by about 25 percent. At the same time, the sensitivity to Reynolds number when nulled has been significantly reduced. Indeed, the influence of Reynolds number is minimal except below a value of $20x10^3$, where the effects of a leading edge separation again appear when the probe is yawed. A futher benefit is the reduced sensitivity of the coefficient to yaw angle. However, some asymmetry can also be seen, though it does appear to be independent of Reynolds number.

The influence of Reynolds number and yaw upon the yaw coefficient is plotted in fig. 15. A comparison of the overall slope of the curves for the new probe (fig. 15b) with those for the old design (fig. 12b) appears to indicate that the sensitivity to yaw is significantly less. In fact, the variation of pressure measured by the yaw tubes (fig. 16) shows that the true sensitivity is unchanged when compared to the forward facing probe (figs. 8b and 9b). The apparent decrease in sensitivity occurs because, as fig. 14 has already shown, the measured pseudo dynamic pressure ($p_1 - p_{av}$) is increased with respect the forward facing probe.

A comparison of figs 15a and 12a, in which the contour intervals represent yaw increments of approximately 2°, reveals that the influence of Reynolds number at high yaw angles and low Reynolds numbers has been reduced. The pressure coefficient results of fig. 16 confirms this. The reduced sensitivity is believed to be because the pressure tubes are located further from the tip and are therefore much less likely to be affected by a leading edge separation bubble at a given Reynolds number. Fig. 15 suggests that the maximum possible error in the measurement of yaw angle is less than 1° throughout the range of Reynolds numbers at all angles of attack but again, the pressure coefficients of the individual holes (fig. 16) imply a greater potential error. At 10° of yaw and for Reynolds numbers between $25x10^3$ and $72x10^3$, the errors indicated by fig. 15 are similar to those noted by Wallen [4] for a probe of identical design.

The results of fig. 14 showed that the change in hole configuration significantly reduces the effect of changes in Reynolds number upon dynamic pressure measurement when the probe is nulled. This is also confirmed by the plots of fig. 16, which indicate a reduced sensitivity of the individual yaw tubes to changes in Reynolds number when the yaw angle is small.

<u>45 and 90°, perpendicular, cone probes.</u> It has been shown that the sensitivity of a 60° cone probe with forward facing holes to changes in Reynolds number is far greater than that of a probe in which the yaw and pitch holes are drilled perpendicular to the surface of the cone. It was also observed that separation of the flow influenced the accuracy of the calibration below a Reynolds number of approximately $20x10^3$. The degree of separation must be related to the cone angle. Therefore, it was decided to calibrate probes with 45° and 90° cone angles. Both of these probes had

yaw and pitch holes which were drilled perpendicular to the surface of the cone.

Figs 17 and 18 present some of the results obtained for the 90° probe. The sensitivity of the yaw calibration to changes in Reynolds number has been futher reduced when compared with either of the 60° probes. There is, for example, only a hint of separation below a Reynolds number of $15x10^3$ at high positive and negative yaw angles in the contours of fig. 17a.

The dynamic pressure coefficient contours of fig. 18a (the contour interval again represents approximately 1 percent of dynamic pressure) may be compared to the those of the 60° probe with perpendicular holes (fig. 15a). For the 90° probe, the sensitivity of the dynamic pressure coefficien to changes in Reynolds number extends over a wider range with the dependence being minimal onl above a Reynolds number of $40x10^3$. The maximum possible error over this wider range is, however, identical to that for the 60° probe suggesting that the 90° probe is much better suited to measurements below $20x10^3$. For the 60° probe, the variation of the coefficient is less rapid in the range from $20x10^3$ to $40x10^3$, so that the converse appears to be true.

It has been noted that yaw coefficient does not exhibit any signs of separation above a Reynolds number of $15x10^3$. The contours of the dynamic pressure coefficient infact suggest that separation exists upto Reynolds numbers of approximately $40x10^3$. This apparent discrepancy arises because the effects of the separation upon the dynamic pressure coefficient are not masked by the changes due to changes in the yaw angle. The variation represents an error of no more than 2.5 percent in the measurement of dynamic pressure.

In part, fig. 19 confirms the trends noted above with regard to changes in cone angle. It shows the effects of yaw and Reynolds number upon the yaw and dynamic pressure coefficients for a 45° con probe. The influence of Reynolds number is most clearly evident in the dynamic pressure contours of fig. 19a. The effects of flow separation at large yaw angles extend to higher Reynolds numbers (approximately $35x10^3$) than for the less sharp probes. When nulled, however, the most importan region of Reynolds number influence is not restricted to values lower that those for the 60° probe. The limit is again approximately $20x10^3$, where the yaw coefficient contours are also distorted as a result of the rapid variations in the psuedo dynamic pressure ($p_1 - p_{av}$).

Although not presented in this paper, the sensitivity of the pressures measured by the individual yaw tubes of the 45° and 90° probes to changes in yaw angle have been examined. For the 45° and 90° probes, these sensitivities were respectively 10 percent less and 10 percent greater than that of the 60° probe. Therefore, at the higher Reynolds numbers, it appears that there is little to chose between the three probes in terms of the true sensitivity of the probes to changes in flow angle. Selection must therefore be made according to the level of accuracy required for the measurement o the dynamic pressure. At the lower Reynolds numbers investigated, the required accuracy of flow angle and dynamic pressure measurements must be weighed against each other.

Effect of Mach Number

So far all of the measurements presented have been obtained at a Mach number of 0.9. To study the influence of compressiblity upon the sensitivity of the calibration coefficients to changes in Reynolds number, the 45° cone probe was recalibrated at Mach 0.5 over the same range of Reynolds numbers.

Some of the results are shown in fig. 20 and may be directly compared with those of fig. 19. The difference between the yaw coefficient contours (figs. 19b and 20b) is only apparent at Reynolds numbers below $17x10^3$. Thus, the yaw coefficient is insensitive to Mach number except at the lowest Reynolds numbers, a result which was later confirmed by calibration of all the probes over range of Mach numbers upto Mach 1.2. In contrast and as might be expected, the dynamic pressur coefficient is not independent of Mach number. However, the general shape of the contours of fig 19a and 20a are similar, suggesting that all of the Reynolds number effects so far encountered nee not be studied at high Mach numbers.

Effect of Turbulence

The previous sections have demonstrated that at least part of the influence of Reynolds number upon probe calibrations is due to the changing nature of the separations which exist at even modest flow angles. This change presumably occurs because of the influence that the Reynolds number exerts upon the transition processes within the separation bubbles. Since free-stream turbulence is also known to influence transition processes, a brief study of the influence of free stream turbulence was undertaken at low speed using the large scale probe pictured in fig. 10.

The probe was calibrated in a low turbulence stream and then again behind a bi-planar turbulence grid with a mesh spacing equal to 85 percent of the probe diameter. The grid size was chosen so as to create turbulence of a simliar relative scale to that occuring in practical environments. The free stream turbulence intensity (streamwise component) was equal to 10 percent for the latter tests.

The results of the two calibrations are shown in fig. 21. The probe is a scale model of the first probe investigated, so that the reader may also compare these results with those of fig. 12. The contour maps of fig. 21 show that the intensity of the turbulence does affect the probe calibration at low Reynolds numbers when, in the case of low turbulence, a separation bubble is known to exist (fig. 10). Thus, free-stream turbulence may influence the accuracy of probes which are sensitive to Reynolds number.

Further Discussion

The results presented above have highlighted two separate Reynolds number effects. The first and simplest is associated with the separation of the flow from the probe tip even at relatively small flow angles. The effects of the separation appear only at relatively low Reynolds numbers (see Table I). It is believed that the Reynolds number affects the transition process and therefore the overall size of the separation bubble. The greater the cone angle of the probe, the lower is the Reynolds number above which the effects of separation are not apparent. Similarly, the closer the pressure holes are to the tip of the probe, the more likely they are to be influenced by the flow separation.

The second Reynolds number effect is most pronounced when the probe is nulled. The effect extends over a greater Reynolds number range than the separation effect and, perhaps more significantly, to higher Reynolds numbers. The measurement of dynamic (or static) pressure is most influenced by this effect. A comparison of the 60° probes with forward facing and with perpendicular pressure holes has shown that the errors caused by operation over a range of Reynolds numbers are greatest in probes of the forward facing type. Although the errors and differences are much smaller, this conclusion is supported by a comparison between the results presented here for a 90° probe with perpendicular holes and the forward facing 90° type of Novak [6]. The former exhibited a 3 percent error in dynamic pressure measurement while the latter produced a 5 percent variation over the same range of Reynolds numbers.

It is not known whether this second effect, which might appropriately be termed a "hole" effect, is due to the changes in open area of the holes, the orientation of the hole axis or both. Nor is the mechanism of the Reynolds number influence understood. However, it must be noted that the pressure holes in a probe such as the forward facing type of fig. 10 occupy a large proportion of the conical surface. For this reason, care has been taken not to refer to the holes as pressure tappings since to do so would infer that the holes themselves do not influence the flow field around the probe. Clearly this is not the case. The holes might well permit flow patterns to develop on a scale which is not disimilar to the scale of the probe and should this occur, the flow might be strongly dependent upon Reynolds number. The flow visualisation of fig. 10 provides evidence that the yaw and pitch holes influence the flow around the probe. Two separation lines can be seen extending from the rear of the pressure hole facing the camera. These separation lines are believed to begin where the flow separates as it moves rearward over the lip created by the forward part of the hole. With separation occuring at the edges of the holes, it is not unreasonable to assume that the flow would be sensitive to small changes in Reynolds number. Indeed, the hypothesis presented here is entirely consistent with the observations of Fransson and Sari [11] who studied the flow around a two dimensional model of a nulled, forward facing probe. They found significant levels unsteadiness in the pressure tubes connected to the yaw holes.

The results presented in this paper have already been compared with those obtained during other investigations of cone probes. It is not possible to make a direct comparison with the data publish for pyramid probes since the probe angles and hole configurations are not the same as those investigated here. However, it is apparent that cone probes are no more sensitive to Reynolds number than pyramid types and that the Reynolds numbers over which the effects occurs are very similar. For example, significant effects of Reynolds number upon the accuracy of yaw measurements made with the 90° forward facing pyramid probe of Krause and Dudzinski [1] are limited to values below approximately 15×10^3, the same limit as observed for the 90° cone probe the present investigation.

It has been noted above that the yaw coefficient is less sensitive to changes in Reynolds number than might be expected from the pressure coefficient data alone. In a turbomachinery environment where the flow vector may be continually changing, the nonlinear response of the individual holes may prevent such a fortuitous combination of events.

CONCLUSIONS

A number of 5-hole cone probes have been calibrated over a range of Reynolds numbers ($7 \times 10^3 <$ Rep $< 80 \times 10^3$) which are typical of those encountered in turbomachinery. The effects of hole configuration, cone angle, compressibility and turbulence intensity have been studied.

Two separate Reynolds number effects have been identified. The first is associated with separation of the flow from the probe body when the probe is at incidence. The effect upon the accuracy of the yaw measurement is limited to Reynolds numbers below 15×10^3 for a 90° cone probe, 20×10^3 for 60° probe and 35×10^3 for a 45° probe. The hole geometry has little effect on these limits but it does influence the magnitude of the Reynolds number sensitivity. The forward facing designs were mo sensitive to changes in Reynolds number.

The second effect is most significant when the probe is nulled and extends to higher Reynolds numbers than does the effect of the leading edge separation. The dependence of the dynamic pressure coefficient upon Reynolds number under these conditions is such that probes with forwa facing pressure holes should not be employed.

A comparison of the probes with pressure holes drilled perpendicular to the conical surface shows that the probe with the largest cone angle (90°) was least sensitive to changes in Reynolds number The variation in yaw coefficient was equivalent to maximum error of 0.7° while the error in the measurement of dynamic pressure was limited to approximately 3 percent. However, the accuracy of dynamic pressure measurement is compromised over a greater range of Reynolds numbers.

An investigation of the effects of compressiblity and free-stream turbulence upon the sensitivity to Reynolds number showed that the basic flow patterns are unaffected by compressiblity whereas changes in free-stream turbulence may have a significant effect.

FINAL COMMENTS

Many facilities do not permit the independent variation of Mach and Reynolds numbers. In such cases, it may be difficult for investigators to prove the Reynolds number insensitivity or otherwise of their probes. However, plots such as those in figs. 12, 15, 17 and 19b may still be produced, even when the Mach number is not constant, since it has been shown that the yaw (and therefore pitch) coefficient is unaffected by changes in Mach number ($M < 1.2$) providing that there is no Reynolds number dependency.

ACKNOWLEDGEMENT

The authors wish to thank Dr. N.C. Baines of Imperial College for his most helpful advice when designing the perforated nozzle which was used for the high speed calibrations.

Our appreciation of the assistance offered by Dr. J-J. Camus of the Whittle Laboratory in the taking of the Schlieren photographs must also be expressed.

REFERENCES

[1] Krause, L.N. and Dudzinski, T.J., "Flow-direction measurement with fixed position probes in subsonic flow over a range of Reynolds numbers," Proc. 15th Int. ISA Aerospace Instrumentation Symp., Las Vegas, May 1969, pp 217-223.

[2] Sitram, N., Lakshminarayana, B., and Ravindranath, A., "Conventional probes for the relative flow measurement in a rotor blade passage", in *Measurement Methods in Rotating Components of Turbomachinery*, ASME 1980.

[3] Smith. A.L. and Adcock, J.B., "Effect of Reynolds number and Mach number on Flow Angularity Probe Sensitivity," N.A.S.A. Technical Memo. TM-87750, 1986.

[4] Wallen, G., "Reynolds number effects of a cone and a wedge type pressure probe," Proc. of 7th Symp. on Measuring Techniques in Transonic and Supersonic Flows in Cascade and Turbomachines, Aachen, Sept. 1983.

[5] Koschel, W. and Pretzsch, P., "Development and investigation of cone-type five-hole probes for small gas turbines," Proc. of 9th Symp. on Measuring Techniques in Transonic and Supersonic Flows in Cascade and Turbomachines, Oxford, Apr. 1988.

[6] Novak, O., "Investigation of the Reynolds number effect of two pressure probes for measurements in turbomachines," Proc. of 7th Symp. on Measuring Techniques in Transonic and Supersonic Flows in Cascade and Turbomachines, Aachen, Sept. 1983.

[7] Gostelow, J.P. and Watson, P.J., "A closed circuit variable density air supply for turbomachinery research," ASME paper 76-GT-62, 1976.

[8] Baines, N.C., "Development of a perforated nozzle for calibrating transonic probes," Proc. of 7th Symp. on Measuring Techniques in Transonic and Supersonic Flows in Cascade and Turbomachines, Aachen, Sept. 1983.

[9] Gaillard, R., " Calibration and use of an ONERA miniature five hole probe," Proc. of 7th Symp. on Measuring Techniques in Transonic and Supersonic Flows in Cascade and Turbomachines, Aachen, Sept. 1983.

[10] Johnson, A.B., "Reynolds number dependence of 5-hole 3 dimensional truncated cone probes," Project Report, Part II Engineering Tripos, Cambridge Univ., Mar. 1985. Supervised by Dr. H.P. Hodson.

[11] Fransson, T. and Sari, I., "Characteristics of Aerodynamic five-hole-probes in transonic and supersonic flow regimes", Proc. 6th Symp. on Measuring Techniques in Transonic and Supersonic Flows in Cascade and Turbomachines, Lyon, Oct. 1981.

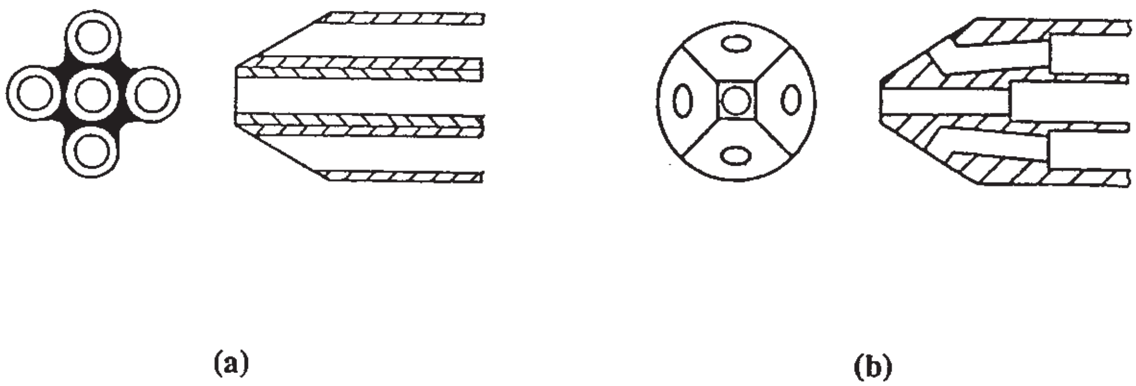

Fig. 1 Pyramid probe types: (a) Forward facing, (b) Perpendicular.

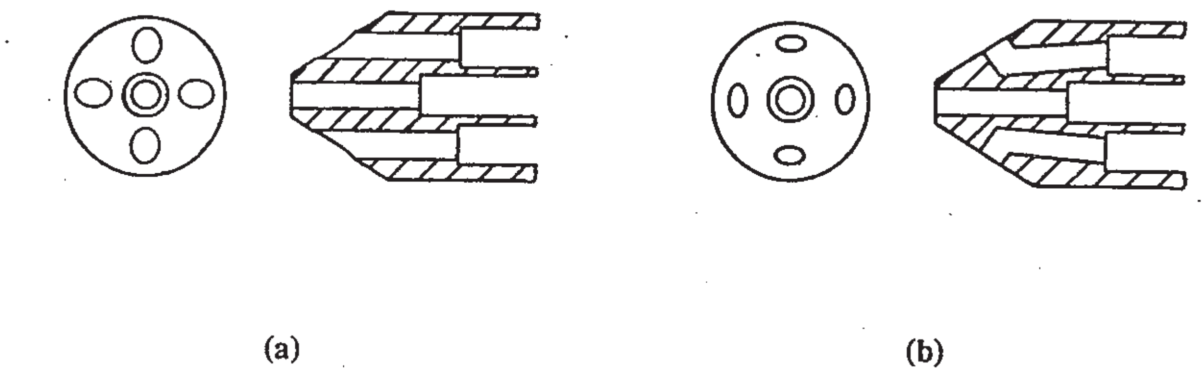

Fig. 2 Conical probe types: (a) Forward facing, (b) Perpendicular.

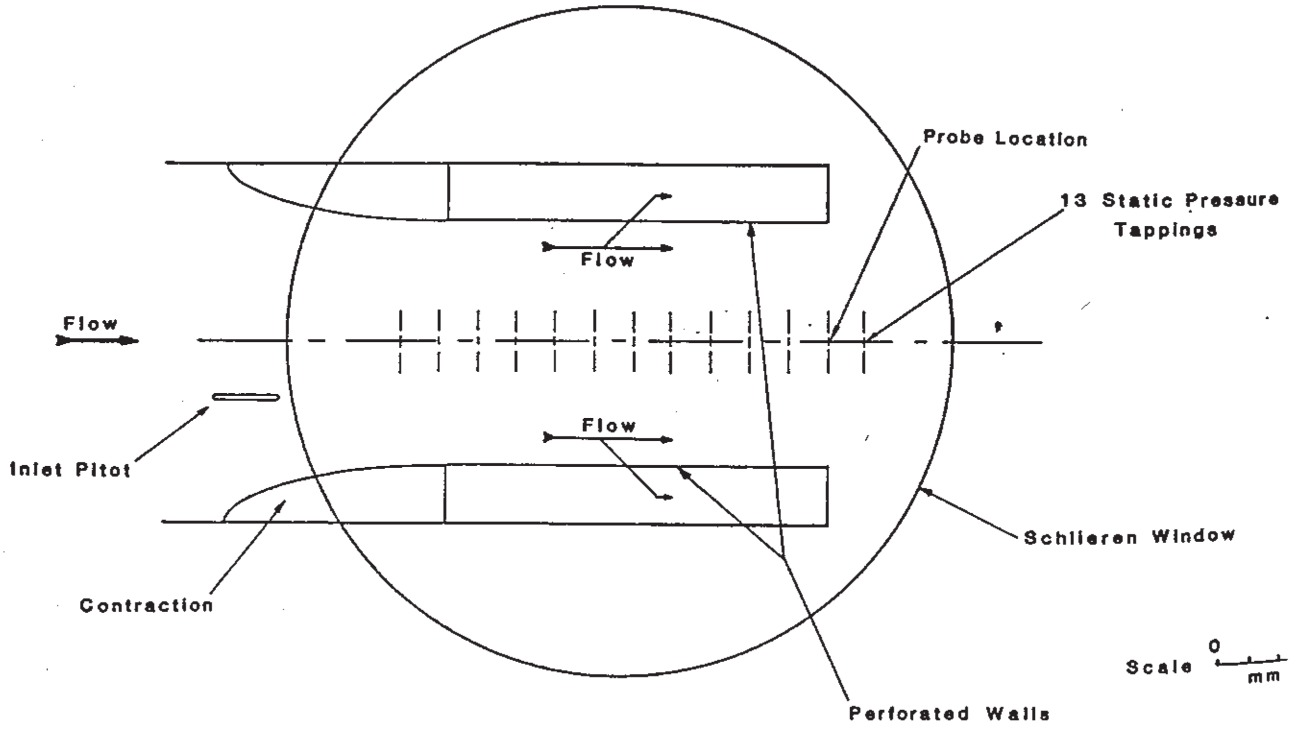

Fig. 3 Elevation of transonic calibration nozzle.

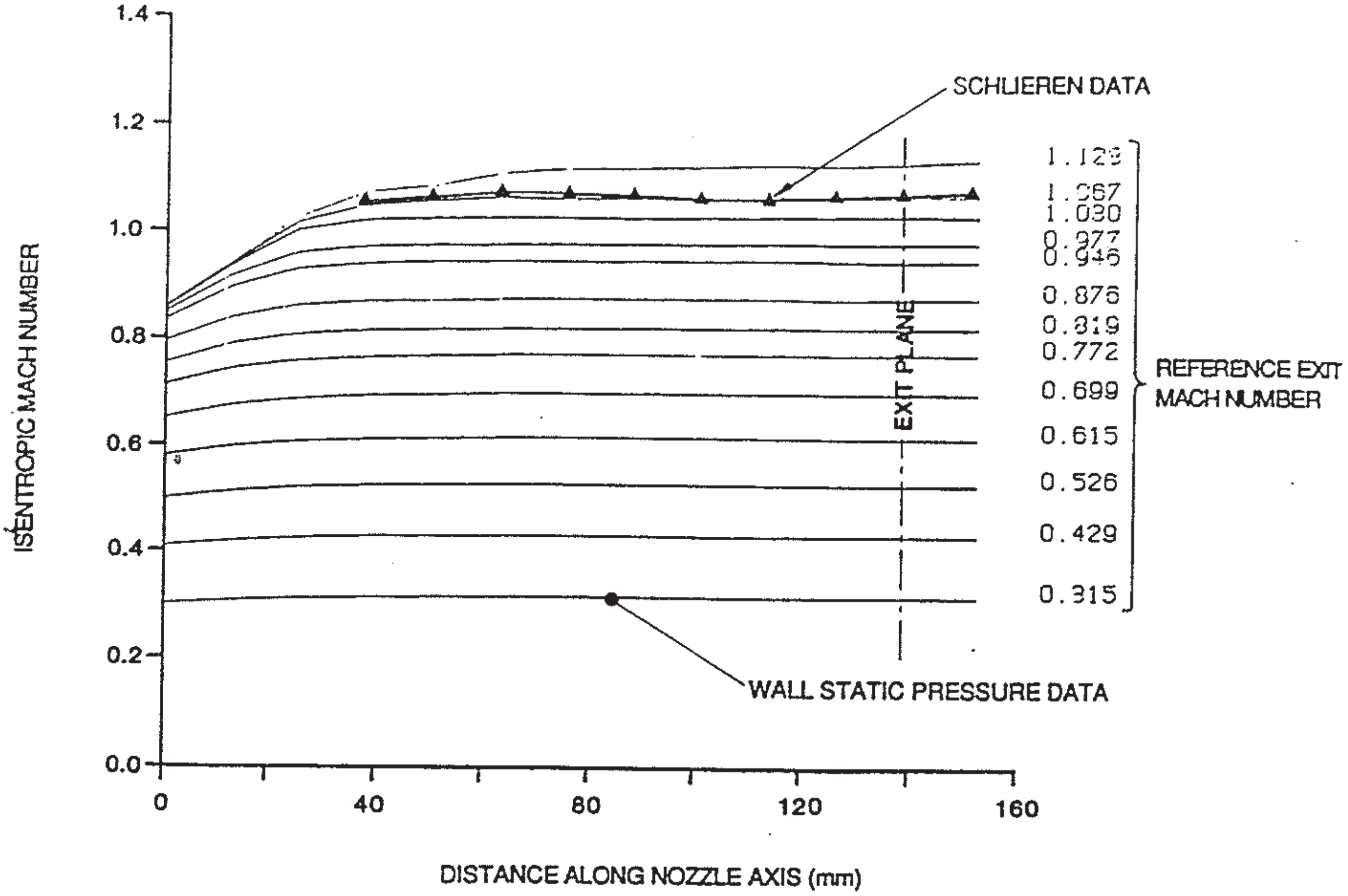

Fig. 4 Isentropic Mach number distributions along axis of calibration nozzle at different back pressures.

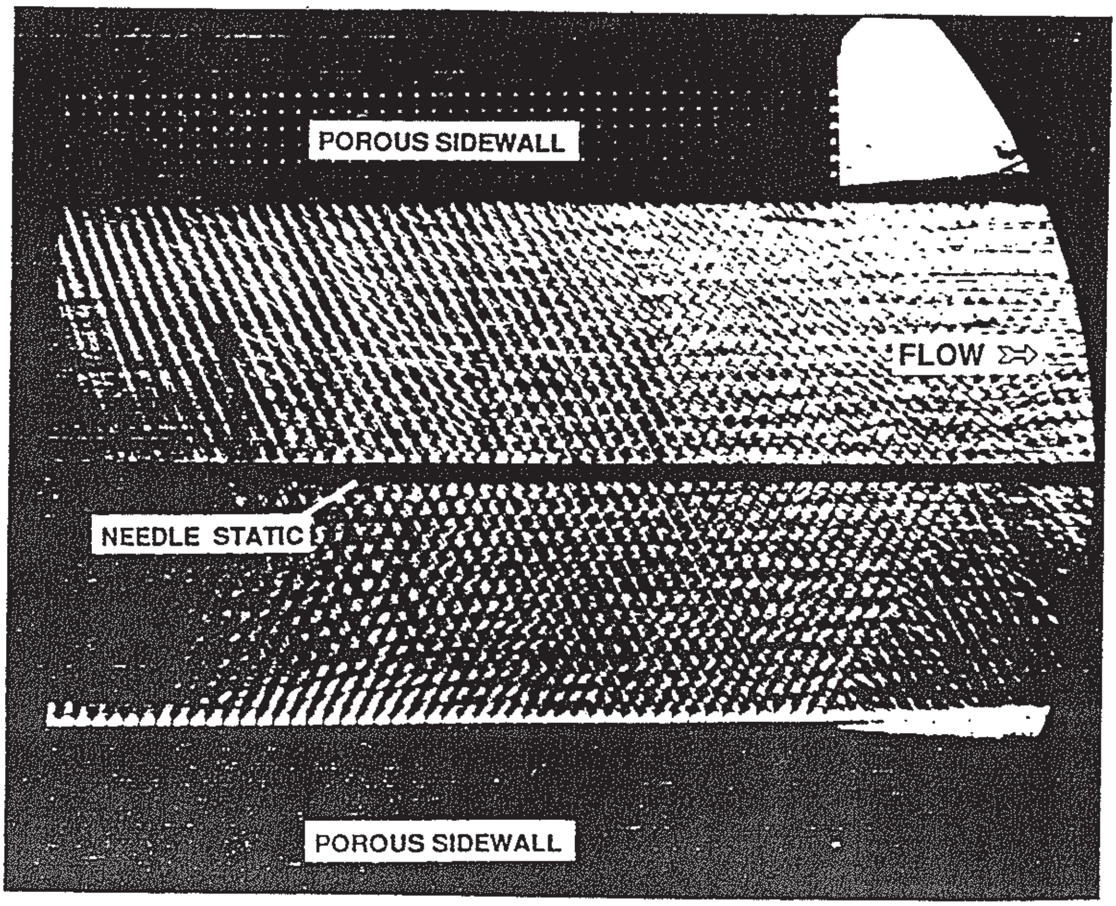

Fig. 5 Schleiren photograph of flow in calibration nozzle at an exit Mach number of 1.08.

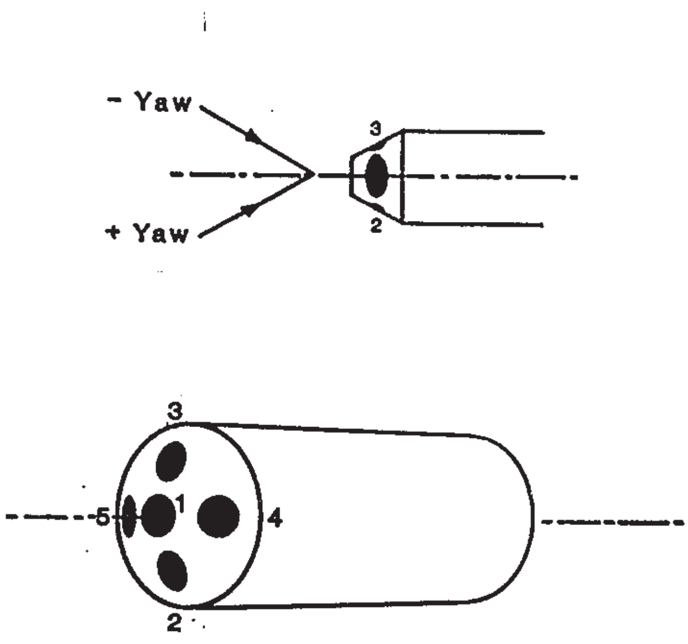

Fig. 6. Hole nomenclature for 5-hole probe.

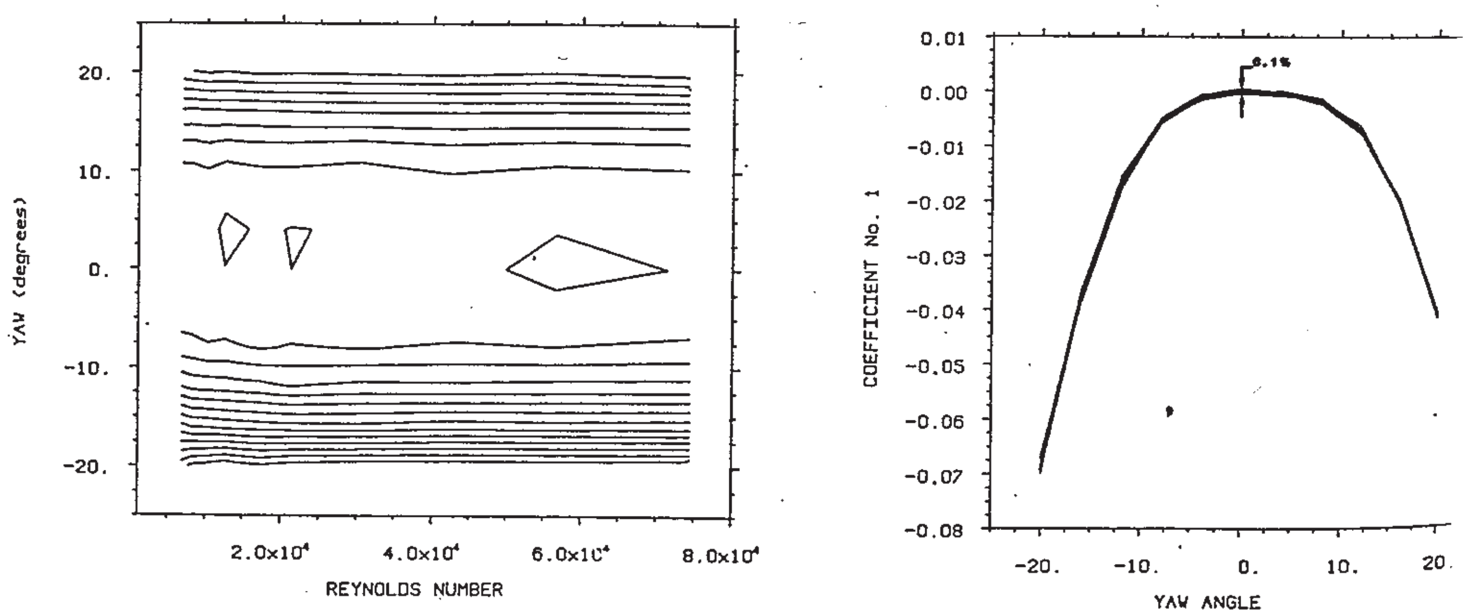

(a) (b)

Fig. 7 Effect of Reynolds number and yaw angle upon pressure coefficient No.1 of 60° forward facing cone probe (No. 501), Mach 0.9:

(a) Contour interval of coefficient = 0.005,
(b) Elevations plotted at Reynolds number intervals of $5x10^3$ commencing at $10x10^3$.

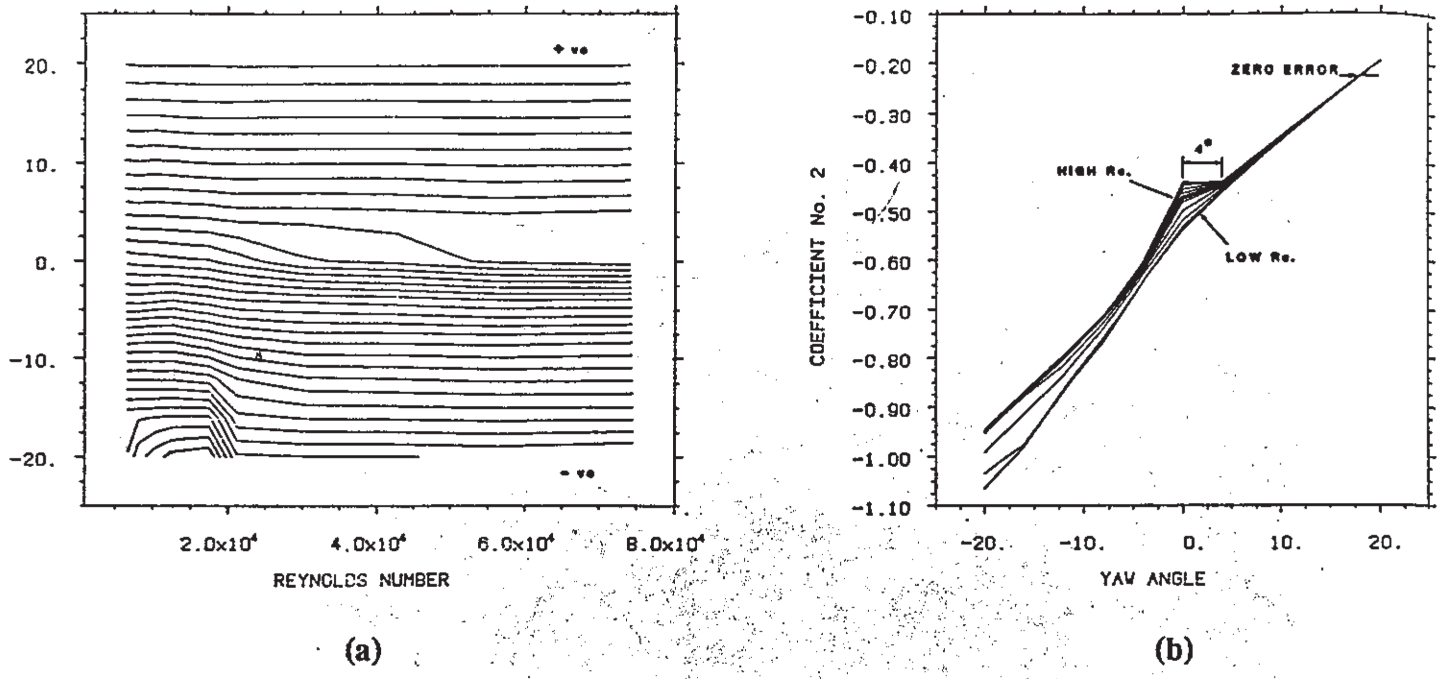

Fig. 8 Effect of Reynolds number and yaw angle upon pressure coefficient No.2 of 60° forward facing cone probe (No. 501), Mach 0.9:

(a) Contour interval of coefficient = 0.025,
(b) Elevations plotted at Reynolds number intervals of $5x10^3$ commencing at $10x10^3$.

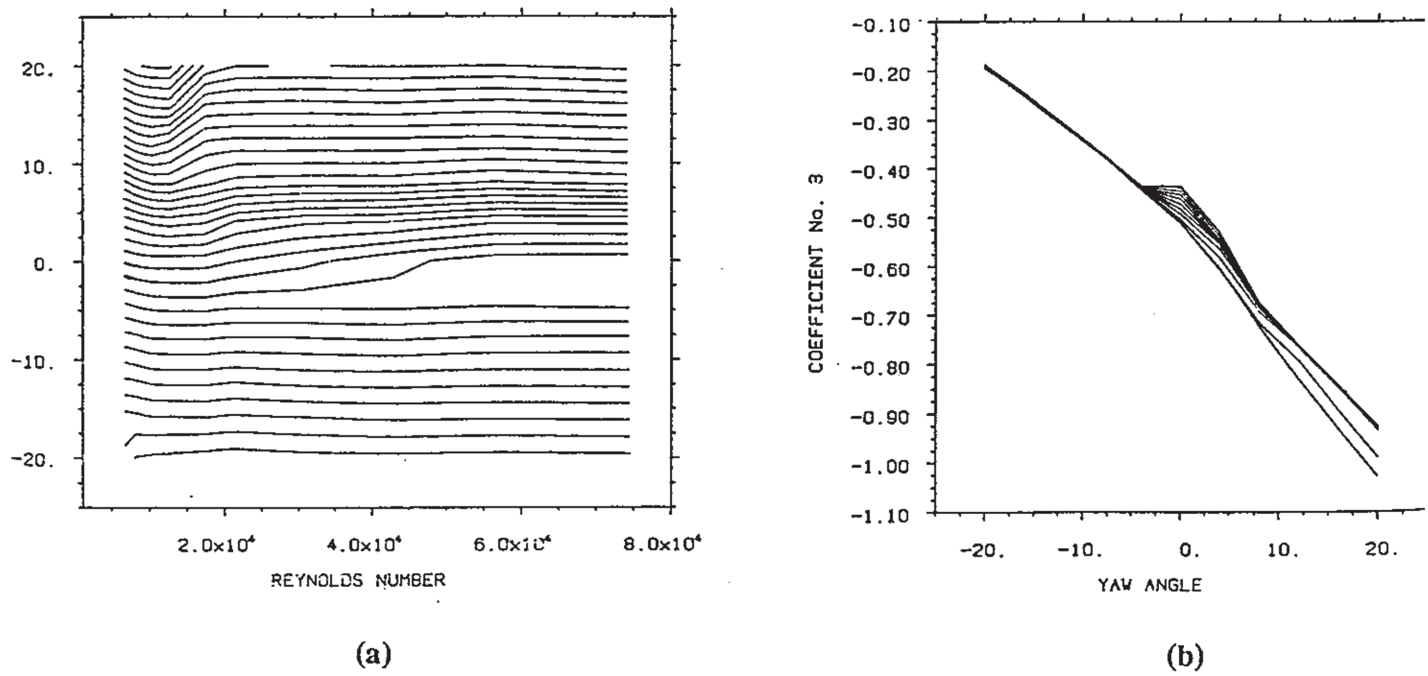

Fig. 9 Effect of Reynolds number and yaw angle upon pressure coefficient No.3 of 60° forward facing cone probe (No. 501), Mach 0.9:

(a) Contour interval of coefficient = 0.025,
(b) Elevations plotted at Reynolds number intervals of $5x10^3$ commencing at $10x10^3$.

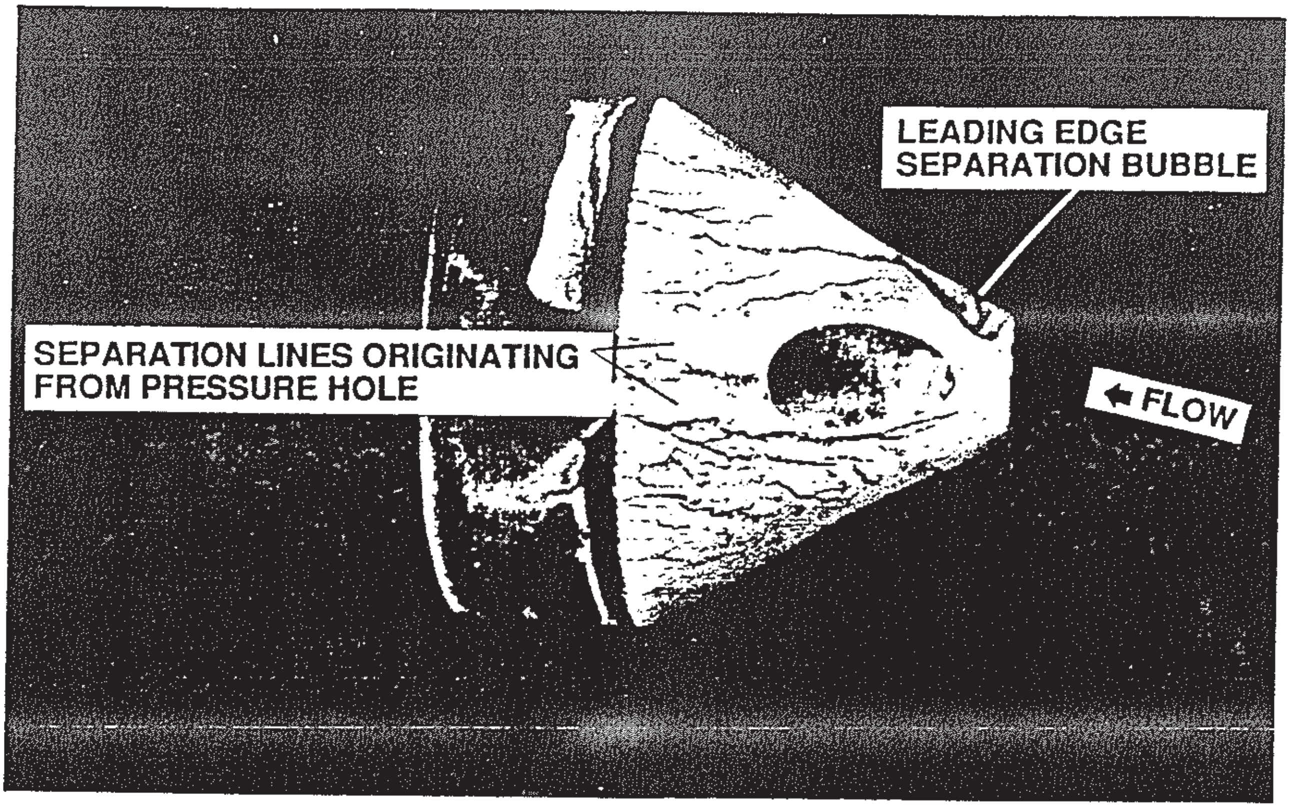

Fig. 10 Oil-and-dye flow visualisation of large scale 60° forward facing cone probe (No. 514) taken from reference [10]: yaw = 8°; pitch = 0° and $Re_p = 13 \times 10^3$

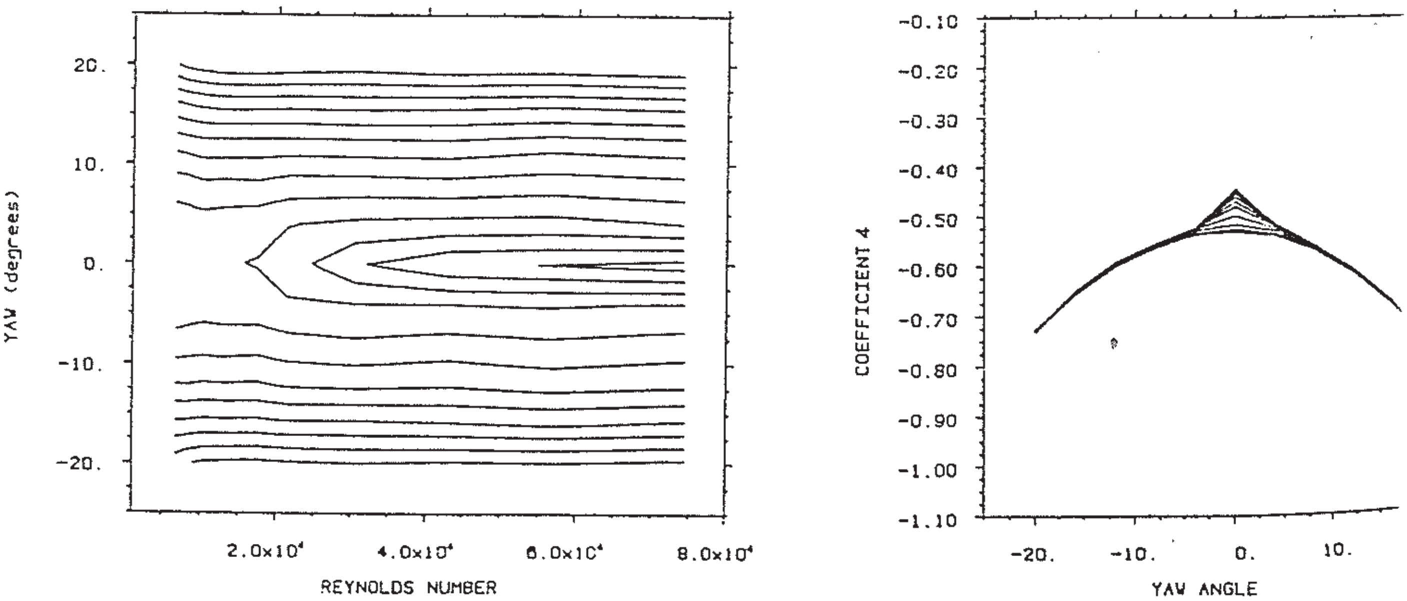

(a) (b)

Fig. 11 Effect of Reynolds number and yaw angle upon pressure coefficient No.4 of 60° forward facing cone probe (No. 501), Mach 0.9:

(a) Contour interval of coefficient = 0.025.
(b) Elevations plotted at Reynolds number intervals of 5×10^3 commencing at 10×10^3

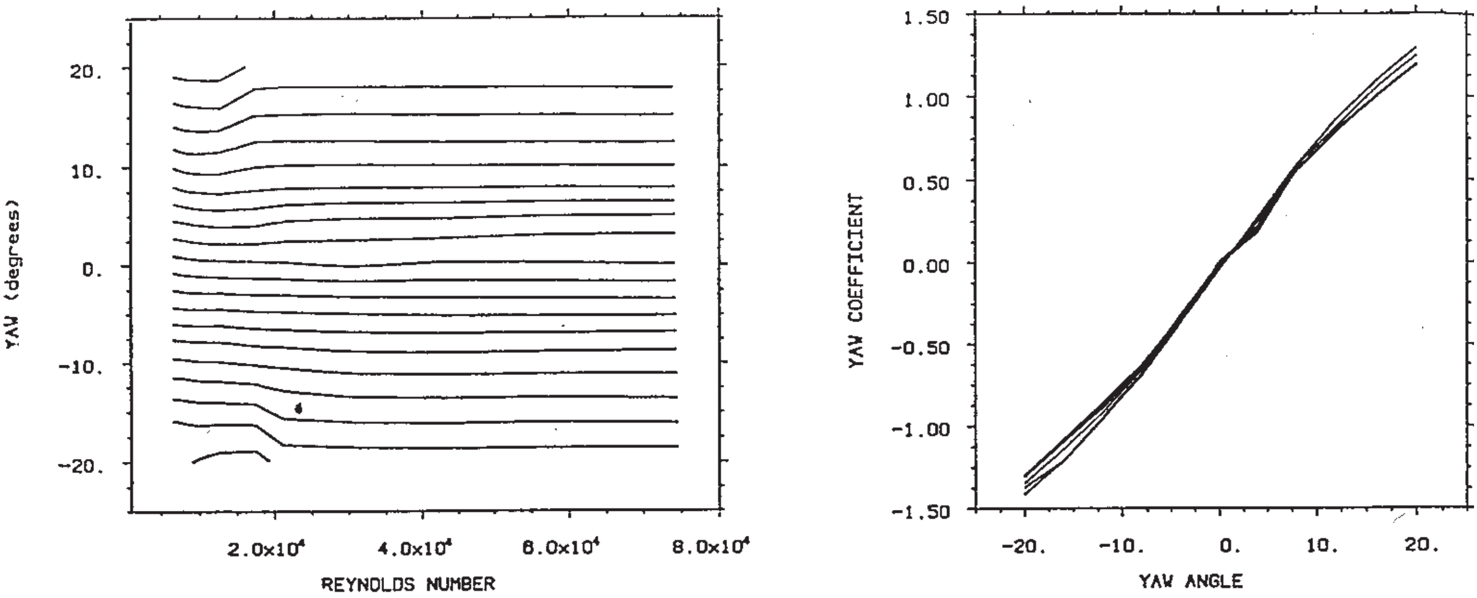

(a) (b)

Fig. 12 Effect of Reynolds number and yaw angle upon yaw coefficient of 60° forward facing cone probe (No. 501), Mach 0.9:
(a) Contour interval of coefficient = 0.136,
(b) Elevations plotted at Reynolds number intervals of $5x10^3$ commencing at $10x10^3$.

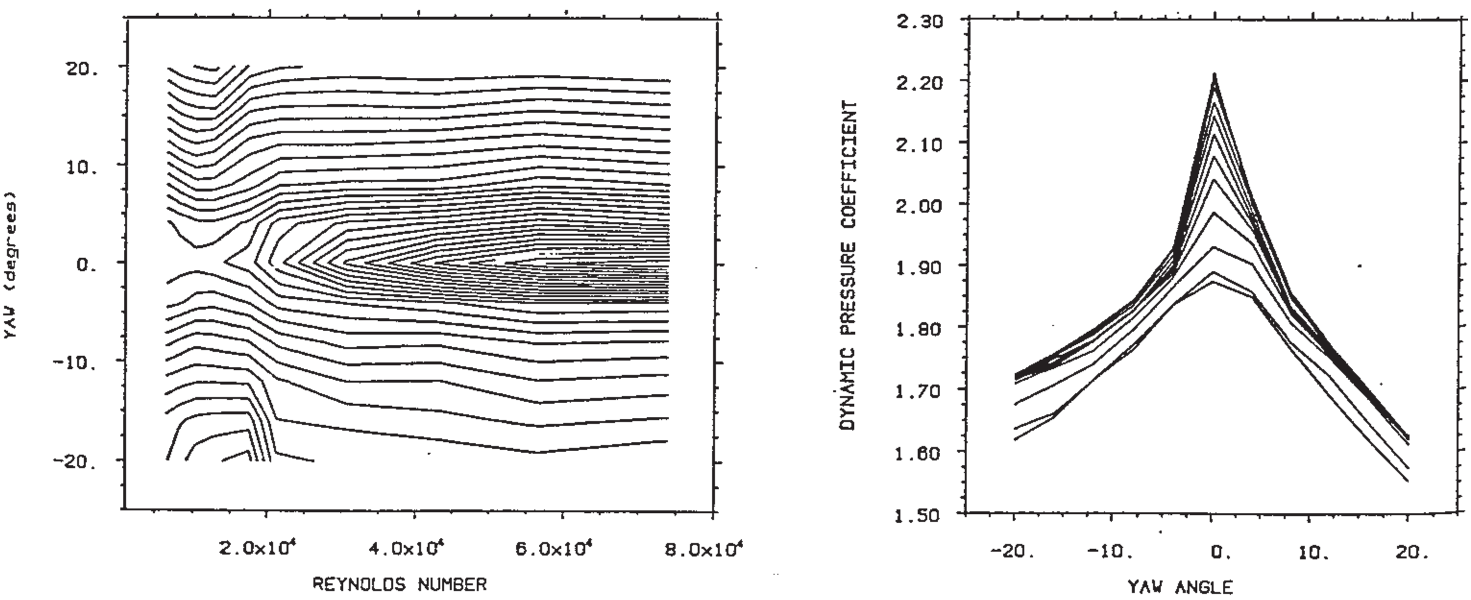

(a) (b)

Fig. 13 Effect of Reynolds number and yaw angle upon dynamic pressure coefficient of 60° forward facing cone probe (No. 501), Mach 0.9:

(a) Contour interval of coefficient = 0.022,
(b) Elevations plotted at Reynolds number intervals of $5x10^3$ commencing at $10x10^3$.

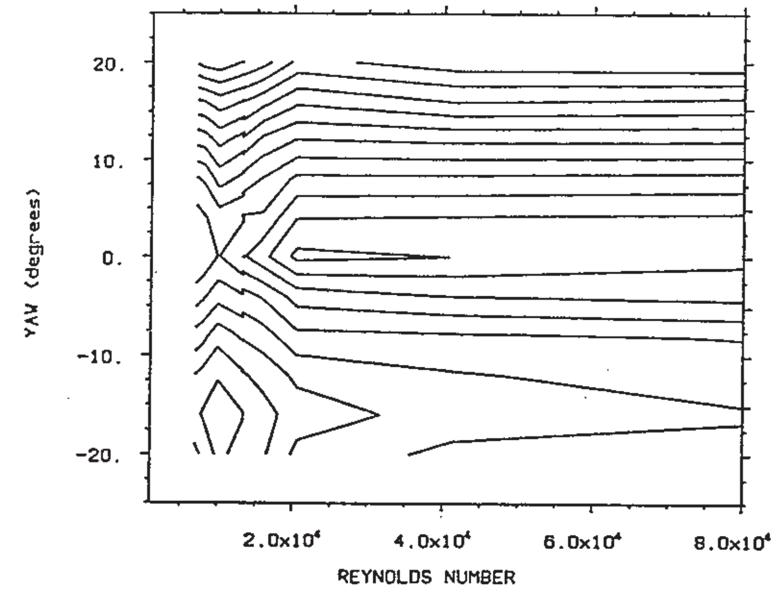

(a)

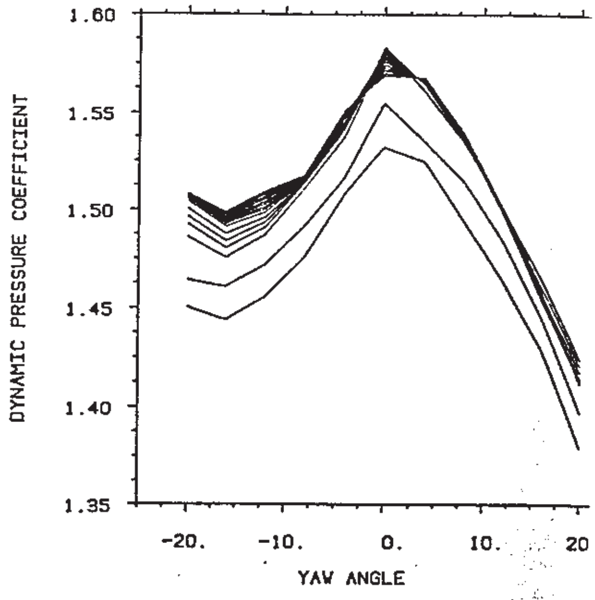

(b)

Fig. 14 Effect of Reynolds number and yaw angle upon dynamic pressure coefficient of 60° perpendicular cone probe (No. 504), Mach 0.9:

(a) Contour interval of coefficient = 0.016,
(b) Elevations plotted at Reynolds number intervals of $5x10^3$ commencing at $10x10^3$.

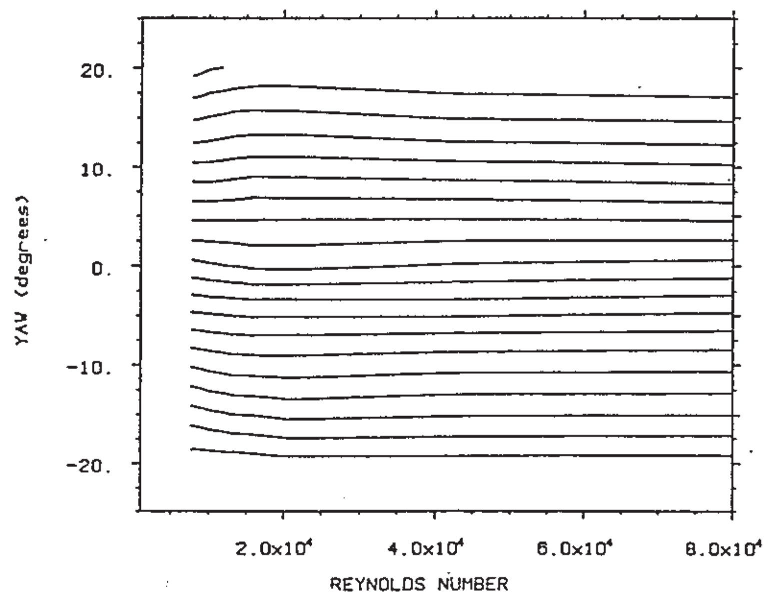

(a)

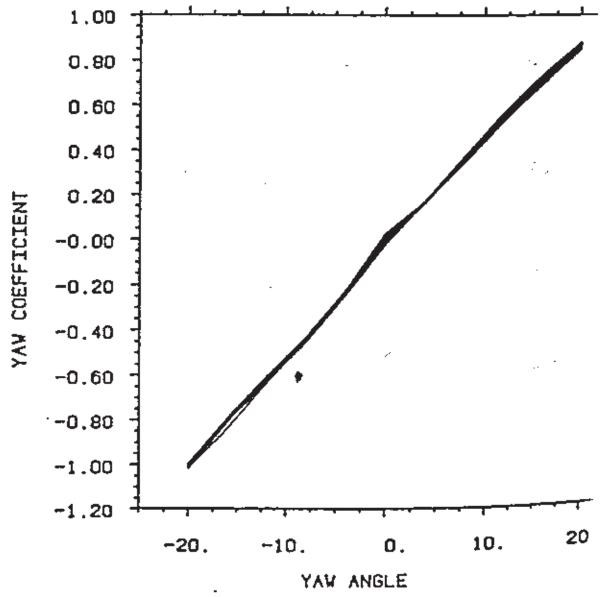

(b)

Fig. 15 Effect of Reynolds number and yaw angle upon yaw coefficient of 60° perpendicular cone probe (No. 504), Mach 0.9:

(a) Contour interval of coefficient = 0.096,
(b) Elevations plotted at Reynolds number intervals of $5x10^3$ commencing at $10x10^3$.

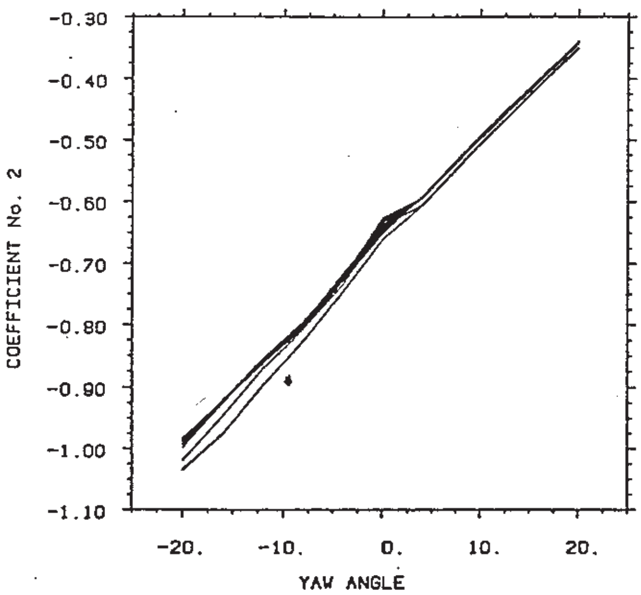

(a)

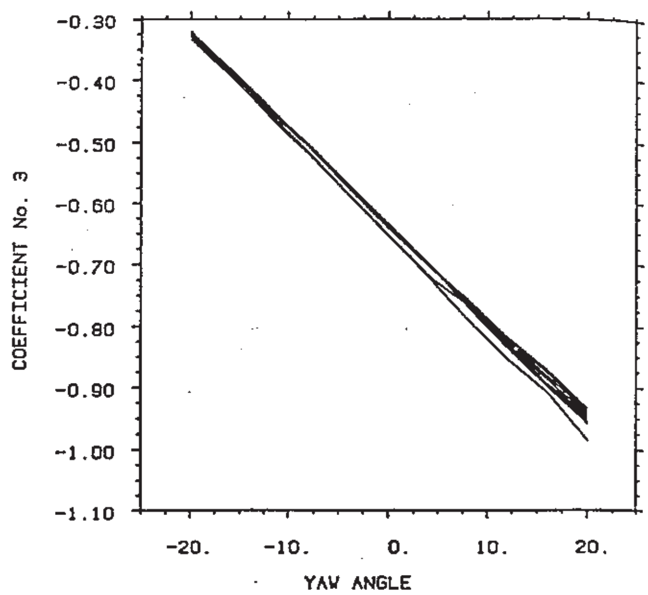

(b)

Fig. 16 Effect of Reynolds number and yaw angle upon pressure coefficients of 60° perpendicular cone probe (No. 504). Elevations plotted at Reynolds number intervals of $5x10^3$ commencing at $10x10^3$:

(a) Pressure coefficient No. 2,
(b) Pressure coefficient No. 3.

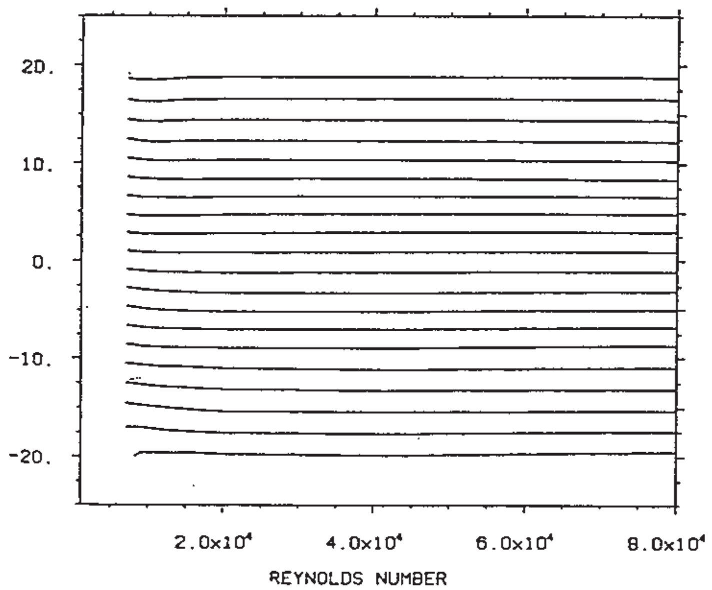

(a)

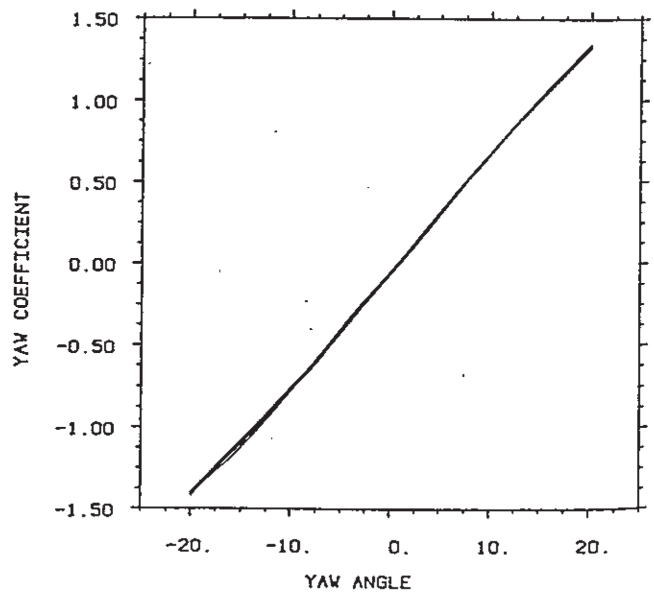

(b)

Fig. 17 Effect of Reynolds number and yaw angle upon yaw coefficient of 90° perpendicular cone probe (No. 506), Mach 0.9:

(a) Contour interval of coefficient = 0.139,
(b) Elevations plotted at Reynolds number intervals of $5x10^3$ commencing at $10x10^3$.

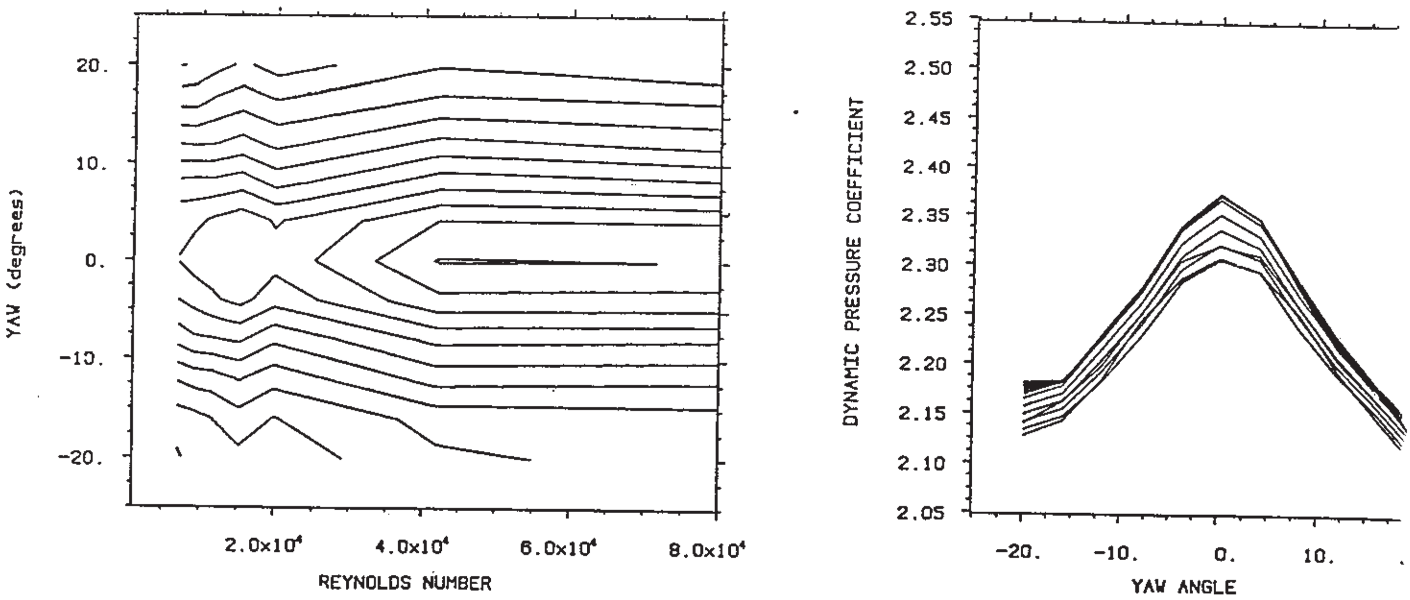

(a) (b)

Fig. 18 Effect of Reynolds number and yaw angle upon dynamic pressure coefficient of 90° perpendicular cone probe (No. 506), Mach 0.9:

(a) Contour interval of coefficient = 0.025,
(b) Elevations plotted at Reynolds number intervals of $5x10^3$ commencing at $10x10^3$.

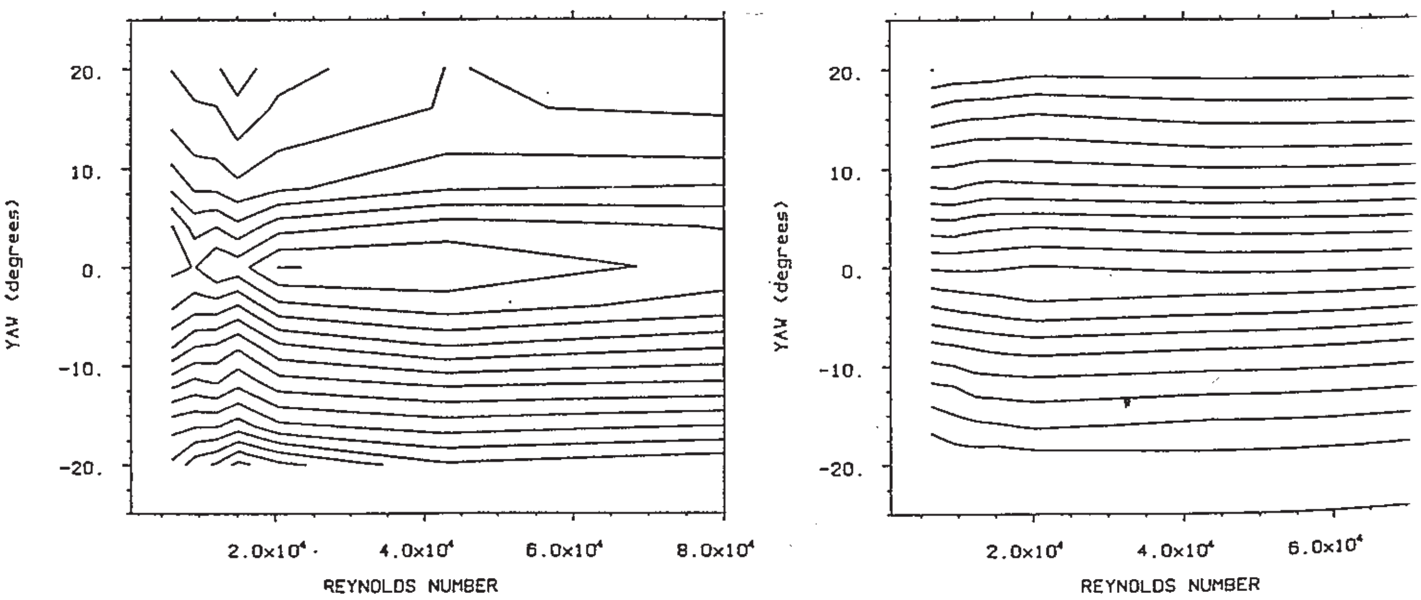

(a) (b)

Fig. 19 Effect of Reynolds number and yaw angle upon dynamic pressure and yaw coefficients of 45° perpendicular cone probe (No. 507), Mach 0.9:

(a) Dynamic pressure coefficient: Contour interval = 0.014,
(b) Yaw coefficient: Contour interval = 0.081.

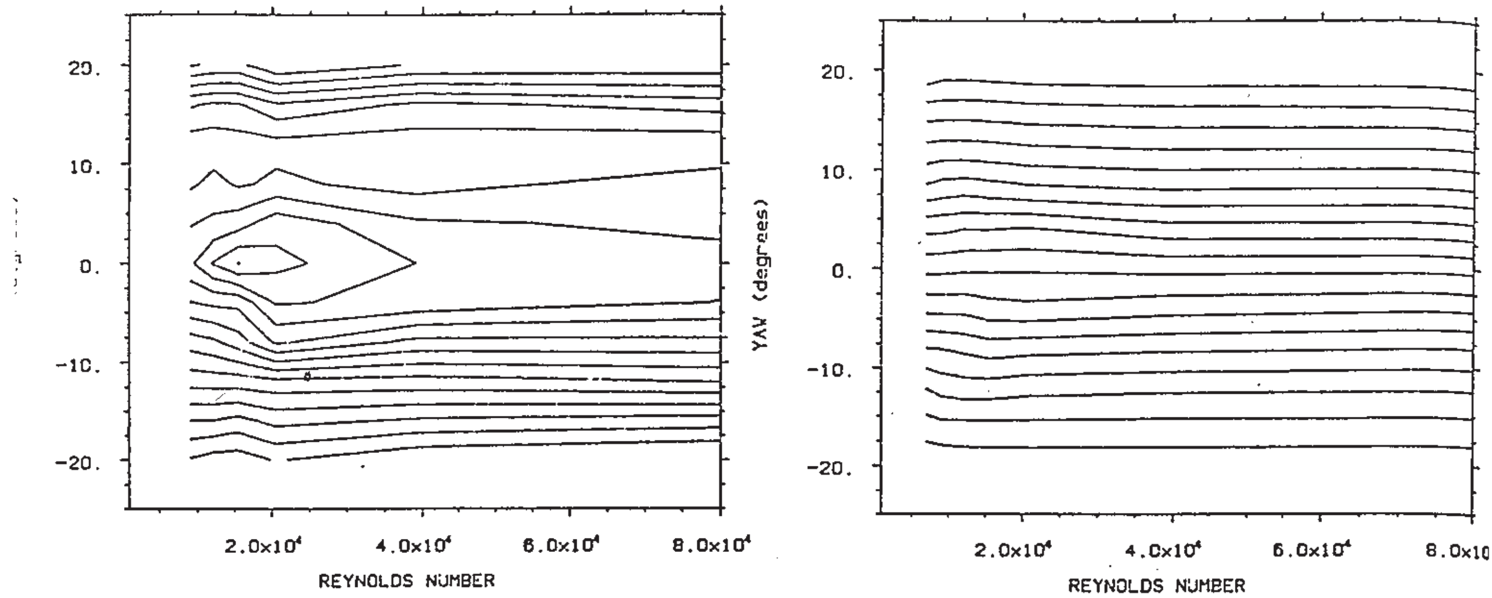

(a) (b)

Fig. 20 Effect of Reynolds number and yaw angle upon yaw coefficient of 60° forward facing cone probe (No. 514) at low speed:

(a) Streamwise turbulence intensity < 0.01%: Contour interval = 0.1,
(b) Streamwise turbulence intensity = 10%: Contour interval = 0.1.

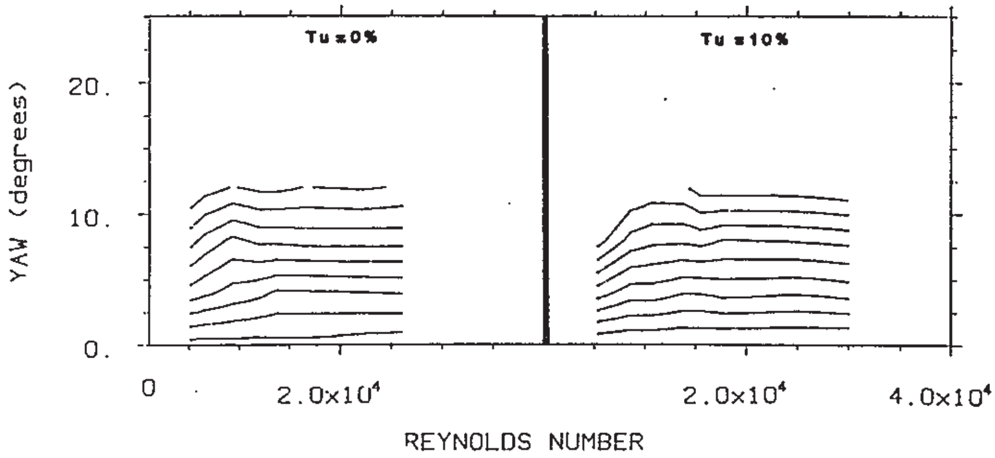

(a) (b)

Fig. 21 Effect of Reynolds number and yaw angle upon yaw coefficient of 60° forward facing cone probe (No. 514) at low speed:

(a) Streamwise turbulence intensity < 0.01%: Contour interval = 0.1,
(b) Streamwise turbulence intensity = 10%: Contour interval = 0.1.